Using Radon-222 as a Naturally Occurring Tracer to investigate the streamflow-groundwater interactions in a typical Mediterranean fluvial-karst landscape: the interdisciplinary case study of the Bussento river (Campania region, Southern Italy).

MICHELE GUIDA[(1,4)*], DOMENICO GUIDA[(2)], DAVIDE GUADAGNUOLO[(1)**], ALBINA CUOMO[(2)], VINCENZO SIERVO[(3)]

[(1)] Department of Physics, University of Salerno, via Ponte Don Melillo, 84084, Fisciano (SA), ITALY

[(2)] Department of Civil Engineering, University of Salerno, via Ponte Don Melillo, 84084, Fisciano (SA), ITALY

[(3)]C.U.G.RI., interUniversity Centre for Applied Research on the Prediction and Prevention of Major Hazards, University of Salerno and University of Naples, Via Ponte don Melillo, 84084 Fisciano (SA), ITALY.

[(4)]I.N.F.N., National Institute for Nuclear and Subnuclear Research, Salerno Branch, University of Salerno, Via Ponte don Melillo, 84084 Fisciano (SA), ITALY.

*miguida@unisa.it, ** davguada@gmail.com

Abstract: - The Bussento river basin, located in the south-east of Campania region, shows interesting issues related to water assessment and management. Complex interactions and exchanges between surface and groundwater exist, influencing also on-shore and off-shore submarine springs. Therefore, gaining river segments from karst groundwater and losing river segments towards the aquifer are recognized. Groundwater protection for drinking domestic use, riverine wild-life conservation and coastal water quality require a progressively optimized knowledge of these interactions. As a support for hydrological modelling tasks, various measurement campaigns have been made along the Bussento river for the acquisition of data about Radon concentration in the river and spring waters, using a radon monitor, Rad7 (Durridge Inc.) , equipped with a water probe and a Rad7H2O to measure radon activity concentration in water. The aim of this preliminary study is to perform an useful methodology for the localization of the contributions of the groundwater along the riverbed, and for their proportional assessment compared with the superficial back return flow.

Key-Words: - Radon, Groundwater, Fluvial Karst Landscape, Hydro-geomorphology, River Drainage Basin

1 Introduction

Surface and groundwater resources assessment represents one of the main issues in socioeconomic planning and management [1, 2, 3, 4] and requires more and more interdisciplinary-based scientific researches, particularly in hydrogeology, hydro-geomorphology and hydrology [5,6].

It is worldwide recognized that global fresh-water resources, stored in rivers, lakes, and aquifers, constitute less than 0.5 % of all the water on the Earth, and therefore, their uses have to be, necessarily, sustainable [7], especially, in the light of a global severe water scarcity scenario forecasted by 2025 [8].

Karst aquifers provide the 25% of the global drinking water resources to the world‘s population and sustain aquatic life in most fluvial systems, providing several ecological services to humans. Being characterized by complex links between surface and groundwater, they turn out to be very vulnerable to contamination and pollution [9].

In Mediterranean environments, karst aquifer groundwater represents more than 98% of the available fresh-water supply and, during summer seasons, feeds perennial streamflow through the aquifer-derived base flow, thus contributing to the total streamflow in a measure of 30% to 70% [10, 11, 12].

An understanding of a given aquifer flow characteristics and its interaction with adjacent surface water resources, turns out to be critical if the total water resource is to be managed sustainably [13, 14].

In order to assess and manage water resources, the European Water Framework Directive 2000/60/EC [15] suggests an integrated approach, taking hydro-geological, hydro-geo-morphological, hydrological, hydro-geochemical, physical and biological contributions into account [16], in particular for groundwater-streamflow interaction assessment and monitoring [17]. Especially in karst Mediterranean landscapes, the interdisciplinarity turns out be fundamental [18, 19, 20]. In fact there are very complex recharge processes and groundwater circulation mechanisms [21, 22, 23].

Determination of the interaction between groundwater and surface water in karst landscape is particularly difficult.

In fact, there are complex hydraulic interconnections of fractures and solution openings in carbonate rocks with basin drainage network. J. V. Brahana and E. F. Hollyday [24] have indicated that dry reaches of streams can be used as indicators of groundwater reservoirs.

In terms of hydro-biological response to hydrologic conditions in karst environments, a number of organisms can be used as indicators of the aquifer-river interactions.

P. Vervier and J. Gibert [25] have quantified the interactions between water, solutes, and organisms at the interface between a stream and a groundwater outlet from karst terrane.

The location of the ecotone showed marked spatial fluctuations according to the prevailing hydrology.

Moreover, interactions were strong during high flows and, on the contrary, negligible, during low flows.

This turns out to be very important in protected areas, as in the study area of the Bussento river basin, which hosts specific destinations for native fish life, regulated by the national environmental legislation.

The use of field measurements to tune and improve physical models is a common practice in environmental control [26,27,28].

In the last decades, a substantial help in providing an answer to the questions of interest in karst hydro-geomorphology and hydrology has been provided by the use of isotopes (stable and unstable) like tracers, both in field investigations as in laboratory analysis [29, 30, 31, 32, 33, 34]. One of the most interesting and promising approach to assess quantitatively the groundwater contributions to streamwaters and seawaters in natural environments, consists in measuring Radon-in-water activity concentrations [35,36, 37].

Therefore, it has been proved that Radon-222 can be an useful natural tracer, because its activity concentrations in groundwater turn out to be typically one order of magnitude or bigger than those ones occurring in surface waters [38].

2 Research Activity

Radon-222 (for sake of simplicity called simply 'Radon' in the following) is a volatile gas with a half-life of 3.8 days, moderately soluble in water and atmosphere.

It is released to groundwater from Radium-226 alpha decay, by means of permanent alpha recoil in micro-pore or fracture walls [39] and progressive dissolution of the aquifer-forming material that supplies more and more soluble Radium-226, subsequently decaying to Radon [40].

Due to its volatility, Radon gas quickly dissipates when exposed to the atmosphere producing a significant disequilibrium between concentrations in surface and groundwater.

From the seminal work of A. Rogers [38], the assessment of spatial-temporal variations in Radon activity concentrations between surface and groundwater [40,41,42] have provided insights in:

1) testing soil infiltration-filtration models [43,44,45,46],
2) performing hydrograph separation [47],
3) calculating residence times [48],
4) interpreting the role of "old water" in non-linear hydrological response of catchments,
5) estimating shallow and deep water mixing [49,50,51,52,53],
6) calculating flow velocities in homogeneous aquifers [54].

For instance, M. Yoneda et al. [55] have used Radon as a tracer to localize the single discrete points of groundwater inflow to a river in Japan. K. K. Ellins et al. [40] have used it to quantify groundwater inputs to a stream in Puerto Rico, and, R. Lee and E. F. Hollyday [42] to assess groundwater contribution to the Carters Creek in Tennessee.

In addition, the use of Radon enables the researchers to trace groundwater migration pathways [56], and to assess the time dependence of groundwater migration processes [57].

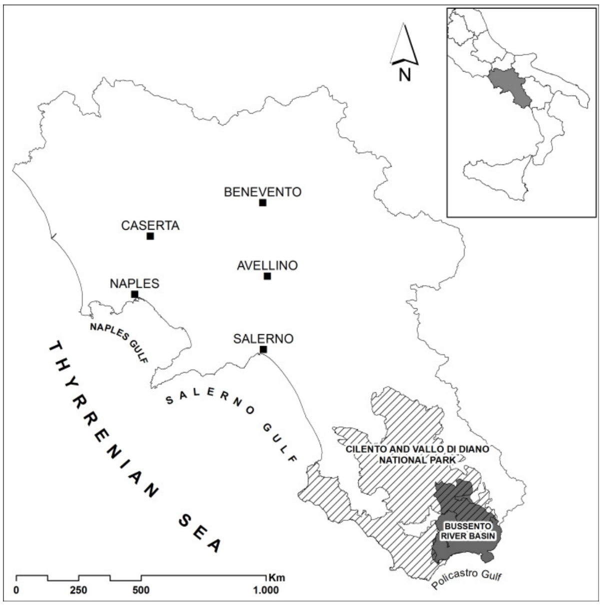

Fig.1 - Location of the study area in Campania region and inside the Cilento and Vallo di Diano National Park.

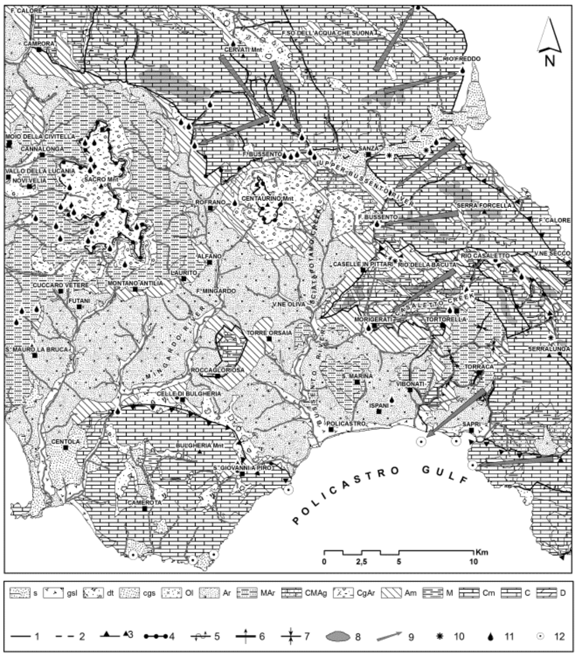

Fig.2 - Hydro-geomorphological map of Bussento river and surrounding.

Infiltration of surface waters from a river to groundwater [49], as well as flow dynamics in a karst system [58], are just few examples of applications, where Radon-based methodology has been successfully used to gain additional information on environmental functioning.

This potential for using Radon, as a suitable aqueous tracer [29], is due to its main characteristics:

1) it occurs naturally in the environment in an ubiquitous way;
2) it behaves like an inert substance;
3) it has a half-life of 3.8 days, differently from other aqueous environmental tracers, like stable isotopes;
4) it is easy to manage, fast to monitor and its measurements inexpensive to be performed.

Usually, Radon-in-water activity concentrations are measured with respect to typical expected or reference values in surface, subsurface and groundwaters.

The measurements can be made through either sampling (batch sampling), performed on fixed volume samples of collected waters from springs or along the riverbed and followed by laboratory analysis, or through continuous monitoring directly in-situ [59].

In the last case, in order to better implement such an approach, it is required the use of simple and inexpensive, field-usable Radon-in-water monitors, with temporal resolutions of hours or less.

There are few commercially available Radon-in-air devices fulfilling those requirements, among which the most commonly used are the “AlphaGuard” (Genitron Instr.) and the “RAD7” (DURRIDGE Co. Inc.).

2.1 Study Area

In this paper, the preliminary results of the experimental investigations on the spatial-temporal variations in Radon activity concentration along the reference segments and reaches of the Bussento river, are illustrated and discussed.

The basin is located inside the Cilento and Vallo di Diano National Park, in the southeastern sector of the Campania region (Southern Italy) (Fig. 1).

It is well known to hydro-geomorphologists and hydrologists for the widespread and unique karstic features [60] (i.e., the sinkhole “La Rupe” and the related “Morigerati resurgence”), and to ecologists for its wildness landscape and wildlife sites (i.e., the otter protection area in the Morigerati WWF Oasis).

In this river basin, the results of previous hydro-geological and hydrological studies [61, 62, 63] indicate a weak correspondence between instrumental registrations and model simulations.

Tab.1 - Climatic characterization of the study area.

Station	Elevation (m a.s.l.)	Mean annual Precipitation (mm)	Mean annual Temperature (°C)	Mean annual Potential Evapotranspiration (mm)	Effective Precipitation (mm)
Morigerati	300	1439	15.9	820	619
Caselle in Pittari	315	1657	15.3	788	869
Casaletto Spartano	310	1811	15.3	789	1022
Sanza	569	1596	12.2	668	928

This is due to the strongly conditioning deep karst circulation in surface hydrological response, with an alternation between gaining river reaches from groundwater, and losing river reaches towards the karst aquifers, and also towards external watershed.

Due to these karst-induced features, the surface and groundwater recharge, circulation and discharge turn out to be very complex.

So, a conceptual hydro-geomorphological model has been developed as a physical context in assessing basin and sub-basin water budget by a semi-distributed hydrological model [64, 65].

As a support for the hydrological modelling tasks, since September 2007, several measurement campaigns have been planned monthly, along sampling stations located either at the beginning or at the end of hydro-geo-morphologically homogeneous fluvial segments or reaches.

For the experimental implementation of the Radon measurements and in compliance with the boundary conditions of the area, where to operate, the most suitable experimental setup turned out to be the portable Radon-in-air analyzer, RAD7 by Durridge Company, Inc. (Bedford, MA, U.S.A.).

It is capable to perform Radon short-lived progenies‘ alpha spectrometry, both directly in–situ, along the riverbed and, offline, in the laboratory, on water sample vials collected during the campaigns.

Besides Radon activity concentrations, chemical and physical parameters (pH, water temperature, dissolved oxygen, TDS, water conductivity, water resistivity, etc..) have been collected.

The instrument used is the multi-parametric HI 9828 (HANNA Instruments S.r.l.).

The Durridge RAD7 Radon Monitor has been extensively used by Bill Burnett and his coworkers in their fundamental work for the assessment of groundwater seepage sites into lakes, rivers, and coastal areas.

These activities have brought to the development of in-situ and continuous radon experimental equipments capable of producing automatic measurements of Radon-222 in surface waters. [66, 67, 68].

During our testing surveys a quick comparison with the Radon-in-Air analyzer AlphaGuard (Genitron Instr.) has been also carried out.

It has been made for one specific monitoring station, confirming the detailed inter-comparison performed by M. Schubert [57, 69].

Synthetically, the objectives of the Radon in-water monitoring program have been:

1) to localize and quantify the contributions of groundwater along the main stream riverbed and banks;
2) to set up an adaptive methodology, based on monthly Radon activity concentration measurements in streamflow and springs, for the baseflow separation from the other streamflow components;
3) to verify the hydrodynamical behaviour of the karst circuits and their influence on streamflow.

The investigation reported in this paper has been performed in order to implement and improve this approach in the conventional regional public practice, to compliance the suggestions derived from the European Water Framework Directive [15] and to apply the methodology to other similar karst-conditioned river basin in Southern Italy.

2.1.1 Hydro-geomorphology of the study area

The Bussento river drainage basin is one of the major and more complex drainage river systems of the southern sector of Campania region, in Southern Italy (Fig. 1).

This complexity is due to the highly hydro-geomorphological conditioning induced by the karst landforms and processes (Fig. 2).

In fact, it is characterized by widely and deeply karst features, like summit karst highlands with dolines and poljes, lowlands with blind valleys, streams disappearing into sinkholes, cave systems, karst-induced groundwater aquifers and gravitational karst-induced “sackungs” [60,70]. The main stream originates from the upland springs of Mt. Cervati (1,888 m asl), one of the highest mountain ridges in Southern Apennines.

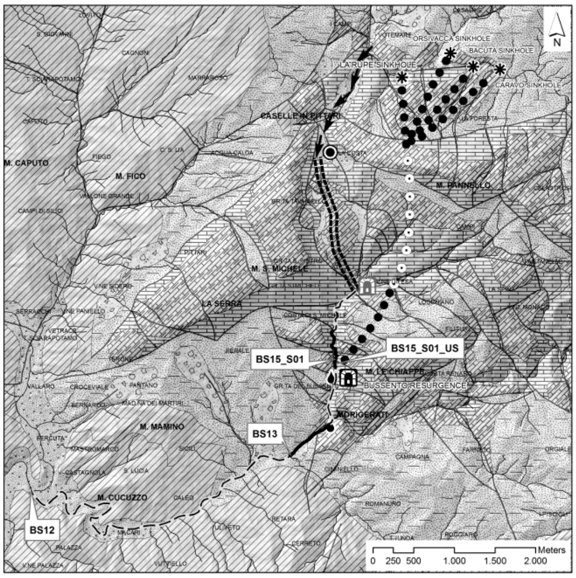

Fig.3 - Detailed hydro-geomorphological map of the study area and related features.

Downstream, the river flows partly in wide alluvial valleys (i.e., Sanza valley) and, partly, carving steep gorges and rapids.

Here a number of springs, delivering fresh water from karst aquifers into the streambed and banks, increase progressively the river discharge.

Near the Caselle in Pittari village, the Bussento river and adjacent neighbour minor creeks flow, respectively, into “La Rupe” (Bussento Upper Cave), Orsivacca and Bacuta-Caravo sinkholes, channelling the entire fluvial surface flow drained in the upper Bussento basin into the hypo-karst cave system and re-emerging a few kilometers downstream, in the neighbourhood of the Morigerati town, from the resurgence, called “Bussento Lower Cave”.

Downstream the resurgence, the Bussento river merges with Bussentino creek, originating from the eastern sector of the drainage basin and flowing along deep canyons and gorges, carved into the meso-cainozoic litho-stratigraphic sequences, prevalently constituted of limestone and marly limestone, referred to the Alburno-Cervati Unit [71].

In the western and southern sectors of the basin (Sciarapotamo creek sub-basin), marly-argillaceous successions of the Liguride and the “Affinità Sicilide Complex” or “parasicilides” [72, 73,74] dominate the hilly landscape, whereas they underlie the arenaceous-conglomerate sequences at Mt. Centaurino [75] (Guida D. et al., 1988).

Downstream the confluence with Sciarapotamo creek, the Bussento river flows as a meander stream in a terraced floodplain and, finally, in the Policastro coastal plain.

In particular, the river drainage sector, which this paper concerns about, refers to the “Morigerati Hydrogeological Structure” [62], comprising the Middle Bussento river Karst System (MBKS). This karst system develops within the carbonate ridge of Mt. S. Michele - Mt. Pannello - Mt. Zepparra , between the four sinkholes located to East of Caselle in Pittari and the final fluvial reach of the gorge located to SE of the Sicilì village (Sicilì bridge), up to the Bussento hydropower plant, just downstream the confluence with Sciarapotamo creek.

In Fig. 3 the detailed hydro-geo-morphological map of the study area, with the hydrogeological complexes and main springs, the hypothesized paleo- and present-day sink-cave-resurgence system, and the river segments and reference reaches of interest, are graphically drawn.

The Middle Bussento segment, comprising the Oasis WWF reach, is located in the Morigerati gorge.

It is a typical epigenetic valley [76, 60], along which groundwater inflows from epikarts spring, conduit spring (Old Mill Spring) and cave spring (Bussento Resurgence) supply a perennial streamflow in a step-and-pool river type [77].

The Middle-lower segment, comprising the Sicilì bridge reach, is located more downstream.

Along the first one, beginning at the end of the Morigerati gorge and stretching to the Sciarapotamo creek confluence, three reaches can be recognized from down-valley:

1) the more downstream, in correspondence of the Bussento Hydropower Plant results a typical riffle-pool river [77], as a meander entrenched in fluvial and strath terraces [78];
2) the second upstream reach, called Bottelli House reach, results in a riffle-pool river along low order alluvial terraces;
3) the third, the above cited Sicilì Bridge reach, a plane bed river slightly entrenched in alluvial terrace and bedrock.

The hydro-geo-morphological setting, above briefly illustrated, induces a very complex surface-groundwater interaction and exchanges.

Tab.2 - Annual minimum streamflow data (m3/s) from published and unpublished river discharge measurements along the cited reference reaches.

Period	1985-1987	1989-1990	1999-2001	2002-2005	2007-2010	Mean
RiverSection	Discharge (m^3/s) (Iaccarino G. et al., 1988)	(courtesy of author D.Guida)	(courtesy of National Park of Cilento)	(courtesy of CUGRI)	(this study)	Discharge (m^3/s)
Upper epikarst springs	0.08	0.12	0.06	0.04	0.05	0.07
Upstream Gorge reach	0.08	0.12	0.06	0.04	0.05	0.07
Lower conduit springs	0.25	0.31	0.22	0.2	0.21	0.238
Intermediate Gorge reach	0.33	0.43	0.28	0.24	0.26	0.308
Intermediate cave resurgence spring	0.35	0.44	0.28	0.23	0.25	0.31
Downstream Gorge reach	0.68	0.88	0.56	0.47	0.51	0.62
Basal fracture springs	0.45	0.38	0.41	0.37	0.39	0.4
MBKS Total Mimimum streamflow	1.13	1.25	0.97	0.84	0.9	1.018

Therefore, groundwater inflows from outside of the hydrological watershed and groundwater outflows towards surrounding drainage systems, frequently occur.

This influences the basin water budget and streamflow regime.

The Bussento river regime is also affected by a very complex hydropower plant system, which retains and diverts the river discharge in the Sabetta reservoir and the Casaletto weirs, respectively, from the upper Bussento river and the Bussentino creek reaches segment to the Lower Bussento fluvial segment.

In order to provide a physical scheme of the complex recharge, storage and routing system of the Middle Bussento karst area, a preliminary, physically-based, conceptual model has been built-up, accounting for an interconnected sequence of geologic substrates, structural discontinuities, type and rate in permeability distribution, recharge areas and discharge points, that collectively attempt a conceptualization of the karst aquifers-river interactions [79, 80, 81, 82].

This model focuses on the variety of hydro-geomorphologic settings and their influences on the streamflow regime.

With reference to the work done by G. Iaccarino et al. [62] and by D. Guida et al. [63] , the conceptual hydro-geomorphological model of the MBKS, contains three nested hydrological domains (Fig. 4):

1) a hydrogeologic domain;
2) a hydro-geo-morphological domain;
3) an aquifer-river domain.

The hydrogeological domain represents the 3-D structure of aquifer, aquitard and aquiclude, conditioning the groundwater circulation and storage.

It is vertically differentiated in the classic subdivision of karst hydro-structures [83]: epikarst, vadose, percolation and saturated or phreatic zones [18].

The last one is hydrodynamically subdivided in cave, conduit and fracture routing system [79].

The hydro-geomorphological domain comprises karst and fluvial landforms and processes, conditioning groundwater recharge (“karst input control”[19]), by means of the infiltration and runoff processes, including:

a) allogenic recharge from surrounding impervious drainage basins into deep and shallow sinking stream infiltration points, and fractured bedrock stream infiltration;
b) autogenic recharge, including sub-soil and bare diffuse epikarst infiltration, endorheic runoff infiltration in dolines and poljes;
c) groundwater discharge (“karst ouput control”[19]), differentiated in the groundwater-river interactions within the aquifer-river domain.

This last comprises the complex interactions between the streambed-springs system, which generally results in a downstream river discharge increase.

It occurrs generally in typical bedrock streams, flowing in gorge and canyons carved in enlarged fractured limestone sequences.

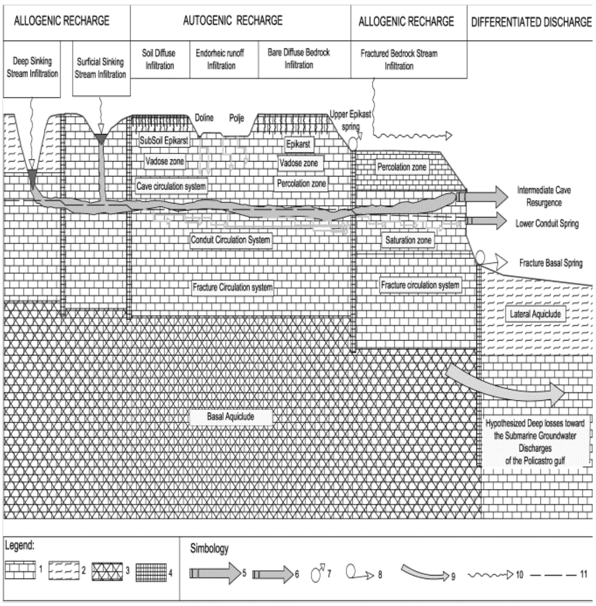

Fig.4 - Conceptual hydro-geomorphological model of the Middle Bussento river Karst System (MBKS).

Following the routing karst system, the springs inflowing into streamlow can be characterized in:

i) upper epikarst springs,
ii) intermediate cave resurgence springs,
iii) lower conduit springs,
iv) basal fracture springs.

Figure 4 highlights, also, the hypothesized deep losses toward the Submarine Groundwater Discharges (SGD), emerging in the Policastro gulf [84], as reported in Fig. 2.

Each of the mentioned components corresponds, in the modelling conceptualization of the scheme, to a linear storage, which releases streamflow as a function of the water storage and of a characteristic delay time.

The characteristic time indicates that there is a delay between the recharge to the system and the output from the system itself, and this delay is greater for deeper aquifers.

The number of storages, each representing, thus, a different process, contributes to the total streamflow through a recharge coefficient, that is a measure of the magnitude of the single storage.

The application of a conceptual model, such as the one briefly described, requires the calibration of the model parameters, and in particular of the characteristic delay time and of the recharge coefficient of each single storage.

In complex catchments, such as the Bussento River System, characterized by a large impact of karstic phenomena, raw streamflow data are not sufficient to the quantification of the contribute and magnitude of the single storage, and, therefore, are not sufficient to calibrate the model.To this aim, the use of Radon activity concentration measurements could represent a valuable future perspective.

The study area is characterized by a typical Mediterranean climatic regime, tending to temperate from the coast to the mountain reliefs. The 50-years (1921-1977) mean annual rainfall and mean annual temperature for historical meteorological stations of Morigerati, Caselle in Pittari, Casaletto Spartano and Sanza, located within the Bussento River watershed, are shown in Table 1 [85].

Since streamflow gauging stations, with long and high quality recorded data, are not available, a characterization of the hydrometric low flow regime is given in Table 2, through data from G. Iaccarino et al. [62], and D. Guida et al. [63], and through discharge data collected during several field campaigns along the river segments of interest (Fig. 3) and from connected groundwater inflows.

3 Materials and Methods

In order to gain useful and effective insights derived from Radon activity concentration measurements and elaborations, improving the MBKS conceptual model above described, monthly measurement campaigns have been performed in the Bussento river basin.

Preliminarly, a Bussento Radon Monitoring Station System (BRMSS) has been established in such a way to be adequate to the locations at the different segment and reach scales of river. The stations, whose coordinate locations have been measured by means of GPS GS20 Professional Data Mapper Leica Geoystems, have been chosen according to their relevance for the study of the interactions between groundwater and surface waters and, then, have been associated to locations either along appropriate points of the main course of the river or in correspondence of the lateral spring inflows.

Each monitoring station has been labeled with an alphanumeric code, beginning with the two letters BS (BS stands for Bussento) followed by a string of bits, containing the station ID number plus a code for distinguishing between spring and river stations (Tab. 3 and Fig. 5).

The format of the identification code has been chosen in the framework of the requirements of the realization of a Relational DataBase, designed specifically for storing all the data related to the assessment of Radon in the territory of Region Campania.

According to the types of stations to be monitored, different measurement techniques, from discrete sampling to continuous measurements, have been tested, both in-situ as in the laboratory, during the preliminary phase of experimentation and testing, aimed to optimize sampling and measurement protocols. In fact, usually, the sampling method is adopted for water samples collected especially from spring locations, where the Radon activity concentrations turn out to be high, while for measurements in surface waters along the river, where lower values can be reasonably expected, a continuous monitoring experimental setup is usually used [59]. The experimental tests have demonstrated a best comparison between data from discrete sampling and continuous monitoring procedures, within the experimental errors.

Therefore, in order to optimize the monitoring campaigns, the sampling measurement approach has been chosen for all type of stations.

The following data acquisition procedure and measurement protocol, consisting of the following steps, have been adopted: sample collection protocol; experimental measurements of the Radon-in-water activity concentrations; evaluation of the effective Radon-in-water activity concentration at the collection time; assessment of the experimental errors.

During the different campaigns, water samples for discrete measurements have been collected, either at some stations along the main course of the river or at some lateral spring inflows. These water samples have been stored in two different types of glass vials: W250 (calibrated volume of 250 ml) and W40 vials (calibrated volume of 40 ml), depending on the value of the Radon activity concentration presumably expected for that location. More specifically, W40 vials have been used for stations with expected high values (about the order of tens of Bq/l), like those characterizing the springs in the Bussento basin, and W250 vials for much lower values (from few Bq/l down to tenth or hundredth of them), like the ones typically occurring in the waters along the streamflow.

In order to be sure that Radon cannot escape from the sample (degassing phenomenon) during the sampling procedure, transportation and offline analysis in the laboratory, both types of vials have been capped with TEFLON lined caps, as quickly as possible after filling them up.

After collecting a sample, each vial has been inverted to check for air bubbles. In presence of air bubbles the sampling procedure has been repeated. The sampling information (code station, date, time and operator‘s name) have been recorded both on the label sample, as, later, stored in the Relational DataBase for Radon Data from Region Campania.Finally, the samples have been stored in a cooler bag for safe transportation and late analysis in the laboratory.

The water samples have been analysed as soon as possible after the collection on the field, in the laboratory, using as equipment, the Radon-in-air analyzer RAD7 (DURRIDGE Company, Inc. - Bedford, MA, U.S.A.), capable to perform Radon short-lived progenies‘ (Polonium-218 and Polonium-214) alpha spectrometry from the air stream maintained through the system with an internal pump.

For these measurements, the RAD7 has been equipped with the accessory kit for sampling measurements in water, RADH20, enabling it to measure radon-in-water, over a wide activity concentration range, from less than about 1 Bq/l up to much greater (orders of magnitude) values than 3 kBq/l [86, 87], with an accurate reading achieved in 30 minutes acquisition data runs.

The RAD7 device, used together with this accessory, contains two built-in measurement protocols for Radon-in-water measurements, for the two types of vials: W250 and W40 protocols. Each run, 30‘ long , consists of 6 cycles, each one 5‘ long.

During the first cycle, the water sample is aerated with air pumped from the internal pump of RAD7. In this way 95% of Radon contained in the water is extracted to air.

In the next one, the system waits for the formation and decay of Polonium-218, while the effective counting of the alpha particles emitted by ^{218}Po starts only in the third cycle and goes on until to the end of the run, when Polonium-218 reaches the secular equilibrium with Radon; thus, enabling the device to compute the Radon activity concentration value.

It must be underlined that the instrumental output, together with the associated alpha spectrum, represents the final value of the Radon activity concentration value in water and not the one occurring in the air.

From our preliminary tests it has turned out to be that, within the experimental errors, the final reading of these sampling measurements provides, for a given Radon monitoring station, a comparable result with a 60‘ acquisition run performed with the continuous measurement setup, consisting of a RAD7 unit and a Radon Water Probe unit, working like an extraction module for Radon from water into the air, also manufactured by DURRIDGE Company, Inc. Exploiting the law of Radon exponential decay, backward-in-time, the data obtained are reevaluated at the time when the water samples have been collected in situ.The overall experimental errors $\sigma_{overall}$ displayed in the following tables and the associated graphs have been calculated by means of the following protocol:

$$\sigma_{overall} = \sqrt{\sigma_{instrument}^2 + \sigma_{sample}^2} \quad (1)$$

where $\sigma_{instrument}$ is the total instrumental error, taking into account also the re-evaluation process of the results at the collection time; σ_{sample} is the overall error we have attributed to the sample collection procedure in-situ, the sample storage, the sample treatment before the measurement in the laboratory, as it cannot be excluded that during the first steps of the experimental procedure, some Radon degassing could have occurred, due to some air entering the vial non perfectly sealed by the TEFLON cap, also, at the moment of the opening of the vials before the laboratory analysis, the non-availability of a cooler, etc. etc.. We have estimated that this kind of error can be reasonably assessed around 10%.

Then, following the measurement protocol made of the previous steps, we have identified some significant portions of the river, which could turn out to be ideal for our analysis and which are described in the following sections. More precisely, the data were collected along two fluvial segments: the former, the Middle Bussento segment, from the Old Mill Spring to the Bussentino creek confluence, and, then, the latter, the Middle-Lower Bussento segment, stretching from this last confluence to the Bussento Hydropower Plant.

Fig.5 – Map of the Bussento Radon Monitoring Station System (BRMSS).

Tab.3 - Radon Monitoring Stations along the Bussento river basin. Bussento Radon Monitoring Station System (BRMSS).

Station Name	Code	X_Coord.	Y_Coord.	Distance from the Coast (m)
Bussento Mouth	BS00	543605.3366	4435295.3874	0
Bussento Mouth Bridge	BS01	543365.5730	4435974.7175	1740
Bussento Railway Bridge	BS02	542247.8301	4438272.0435	3680
Vallonaro Creek	BS03	541834.8402	4440099.9059	6200
Sciarapotamo Creek	BS04	543412.8693	4442664.5218	10930
Bussento Hydropower	BS12	543583.6737	4442368.8007	10246
Sicilì Bridge	BS13	546446.5601	4442939.8484	14100
Casaletto Creek	BS14	553475.0352	4445318.3639	22717
Old Watermill Spring	BS15-S01	546915.6349	4444081.9437	15580
Ciciniello Creek	BS16	545934.8916	4449803.4248	22300
Sabetta Reservoir	BS17	547207.9202	4449424.2903	20900
Acquevive Bridge	BS18	548000.0954	4451699.0969	23534
Farnetani Bridge	BS19	546973.6582	4452744.0284	25550
L'Abate Bridge	BS20	544406.0243	4453604.0162	28460
Inferno Creek Bridge	BS21	543083.6774	4454695.1836	30300
Persico Bridge	BS22	543049.7711	4454630.4533	30095
Bussentino Bridge	BS23	548065.3782	4443510.8961	15995
Melette Spring	BS24-S01	557102.7175	4446756.1804	28734
Bacuta Sinkhole	BS25	548948.4602	4447695.8382	20500

4 Results and Discussion

The Radon activity concentration data, acquired as reported above, have been arranged in relation to the fluvial level hierarchy and scale analysis: firstly, at segment scale, managing the data collected only from the main stations; secondly, at reach scale, including also the data from the complementary stations.

Finally, as experimental support to improve the MBKS conceptual model, the results of the Radon activity concentration from the karst spring monitored have been explained and discussed.

4.1 River segment scale analysis

The first river segment, the Middle Bussento Segment, starting from Old Mill Spring to Bussentino creek confluence gorge, comprises, from upstream, the following stations: BS15_S01_US (Upstream Old Mill Spring Station), BS15_S01_01 and BS15_S01_03 (below Old Mill Spring Station), BS15_S01_DS (downstream Old Mill Spring Station).

The second river segment, the Middle-lower Bussento, starts from the above cited confluence gorge to the Bussento Hydropower Plant, comprising, from upstream, the following stations: BS13_US, BS13_01, BS13, BS13_DS and BS12, with the numerous groundwater inflows from the bank and bed fracture along the uppermost segment reach.

The groundwater inflows from the Cillito spring group are represented with the main spring code BS13_S01.

Tables 4 and 5 contain all the Radon activity concentration data from some selected stations on the two river segments of interest together the main contributing springs.

The correlation between the Radon activity concentration mean values vs. the topographic distance of the stations, monitored along the two segments, are graphically displayed in Figg. 6 and 7, highlighting the locations of the Radon high-content inflows from the main spring stations.

In Table 4 the BS25 (Bacuta Sinkhole Station) has been added to compare the Radon activity concentration in streamwater ingoing the MBKS, with the unique groundwater inflow into streamflow from the karst conduit Old Mill Spring (spring code: BS15_S01).

Data analysis at segment scale highlights the spatial variations of Radon activity concentration, detected along the medium and medium-lower Bussento river segments.

The following considerations can be made:

i) the in-water variations of Radon activity concentration vs. the river long profile detect clearly the location of the surface-groundwater interactions, also where no discharge increments result from quantitative surveys (see BS15_S01_US and BS13_DS values);

ii) the linear extension downstream of the groundwater influx can be roughly defined, strictly related to the magnitude of the groundwater inflow and hydraulic condition of each reach;

iii) the approximate streamflow reference base value in the Radon activity concentration for the Bussento river can be estimated, corresponding to the lower values detected from BS12 station (mean value: 0.7 Bq/l) and BS25 station (mean value: 0.3 Bq/l).

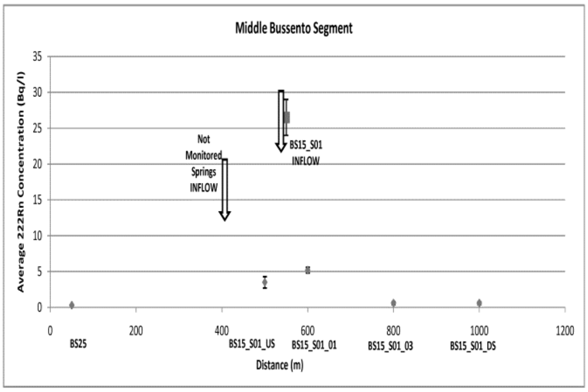

Fig.6 - Average Radon activity concentration values measured along the Middle Bussento segment

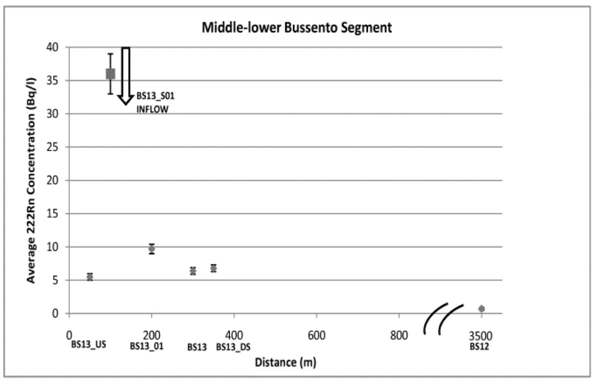

Fig.7 - Average Radon activity concentration values measured along the Middle-lower Bussento segment.

Tab.4 - Radon activity concentration values measured along the Middle Bussento segment.

STATIONS	BS25	BS15_S01_US	BS15_S01	BS15_S01_01	BS15_S01_03	BS15_S01_DS
Measurement Campaign	Radon activity Concentration (Bq/l)	Radon activity Concentration (Bq/l)	Radon activity Concentration (Bq/l)	Radon activity Concentration (Bq/l)	Radon activity Concentration (Bq/l)	Radon activity Concentration (Bq/l)
Sept. 07	N.M.	N.M.	**25 ± 2**	N.M.	N.M.	N.M.
Dec. 07	N.M.	N.M.	**33 ± 3**	N.M.	N.M.	N.M.
Jan. 08	**0.4 ± 0.1**	**6.1 ± 1.6**	**26.5 ± 6.5**	N.M.	N.M.	**2.0 ± 1.7**
Feb. 08	**0.2 ± 0.1**	**0.9 ± 0.4**	**28 ± 3**	**3.7 ± 0.4**	**0.4 ± 0.2**	**0.2 ± 0.1**
Mar. 08	N.M.	**0.6 ± 0.4**	**7 ± 6**	**0.4 ± 0.1**	**0.6 ± 0.3**	**0.8 ± 0.5**
April 08	**0.3 ± 0.2**	**1.6 ± 0.1**	**33.5 ± 6.5**	**3.7 ± 0.9**	**0.4 ± 0.3**	**0.8 ± 0.1**
May 08	N.M.	**1.7 ± 0.8**	**17.5 ± 3.5**	**8.7 ± 0.8**	**0.9 ± 0.5**	**0.6 ± 0.3**
June 08	N.M.	**6.5 ± 1.2**	**25.5 ± 3.5**	**8.2 ± 1.4**	**0.8 ± 0.3**	**0.3 ± 0.2**
Oct. 08	N.M.	**6.3 ± 1.3**	**21.5 ± 5.0**	N.M.	N.M.	**0.2 ± 0.1**
Dec. 08	N.M.	**4.0 ± 1.0**	**28 ± 5**	**6.9 ± 0.5**	**0.4 ± 0.4**	**0.5 ± 0.3**

Tab.5 - Radon activity concentration values measured along the Middle-Lower Bussento segment

STATIONS	BS13_US	BS13_S01	BS13_01	BS13	BS13_DS	BS12
Measurement Campaign	222Rn Concentration (Bq/l)	222Rn Concentration (Bq/l)	222Rn Concentration (Bq/l)	222Rn Concentration (Bq/l)	222Rn Concentration (Bq/l)	222Rn Concentration (Bq/l)
Sept. 07	N.M.	**28 ± 2**	N.M.	**4.5 ± 0.8**	N.M.	N.M.
Dec.07	N.M.	**45 ± 8**	N.M.	**5.0 ± 0.8**	N.M.	**0.9 ± 0.2**
January 08	**4.3 ± 1.2**	**35 ± 6**	**6.7 ± 0.6**	**5.2 ± 1.1**	**7.0 ± 1.4**	**0.7 ± 0.3**
February 08	**3.2 ± 0.5**	**33.7 ± 1.2**	**8.9 ± 0.9**	**5.1 ± 0.6**	**7.2 ± 0.8**	**1.1 ± 0.4**
March 08	**0.9 ± 0.5**	No Measure	**5.0 ± 0.5**	**1.0 ± 0.5**	**1.2 ± 0.3**	**0.6 ± 0.4**
April 08	**7.6 ± 1.3**	**35.5 ± 7.5**	**12.2 ± 1.8**	**6.9 ± 0.6**	**8.0 ± 0.8**	**0.8 ± 0.5**
May 08	No Measure	**37 ± 9**	No Measure	**8.7 ± 1.7**	**9.1 ± 1.8**	No Measure
June 08	**8.8 ± 1.5**	No Measure	**14 ± 4**	**9.4 ± 1.2**	**8 ± 2**	No Measure
October 08	**9.0 ± 0.8**	**35.5 ± 4.5**	**11.3 ± 1.5**	**7.7 ± 1.0**	**7.6 ± 0.9**	**0.3 ± 0.3**
December 08	**4.5 ± 0.3**	**36.5 ± 3.5**	**10 ± 2**	**5.4 ± 0.6**	**6.2 ± 1.1**	**0.6 ± 0.3**

Tab.6 - Radon measurements data from all the stations along the Middle-lower Bussento Segment.

Stations	BS13_US	BS13_03	BS13_02	BS13_01	BS13_00	BS13	BS13_DS	BS13_DS_J_DS	BS12
Measure Campaign	222Rn Concentration (Bq/l)	222Rn Concentration (Bq/l)	222Rn Concentration (Bq/l)	222Rn Concentration (Bq/l)	222Rn Concentration (Bq/l)	222Rn Concentration (Bq/l)	222Rn Concentration (Bq/l)	222Rn Concentration (Bq/l)	222Rn Concentration (Bq/l)
Sep 07	No Measure	No Measure	No Measure	No Measure	No Measure	**4.5 ± 0.8**	No Measure	No Measure	**1.1 ± 0.3**
Dec 07	No Measure	No Measure	No Measure	No Measure	No Measure	**5.0 ± 0.8**	No Measure	No Measure	**0.9 ± 0.2**
Jan 08	**4.3 ± 1.2**	**5.0 ± 0.6**	**6.5 ± 1.3**	**6.7 ± 0.6**	**5.3 ± 1.5**	**5.2 ± 1.1**	**7.0 ± 1.4**	**5.1 ± 0.5**	**0.7 ± 0.3**
Feb 08	**3.2 ± 0.5**	**6.6 ± 1.0**	**7.7 ± 0.9**	**8.9 ± 0.9**	**7.9 ± 0.8**	**5.1 ± 0.6**	**7.2 ± 0.8**	**6.1 ± 0.9**	**1.1 ± 0.4**
Mar 08	**0.9 ± 0.5**	**2.7 ± 0.5**	**3.4 ± 0.7**	**5.0 ± 0.5**	**1.9 ± 0.2**	**1.0 ± 0.5**	**1.2 ± 0.6**	**1.1 ± 0.5**	**0.6 ± 0.4**
Means 1	**2.2**	**3.9**	**5.2**	**6.2**	**4.9**	**3.4**	**3.8**	**3.5**	**0.89**
StDev 1	**0.3**	**0.3**	**0.5**	**0.3**	**0.5**	**0.3**	**0.4**	**0.3**	**0.12**
Var 1	**0.11**	**0.13**	**0.25**	**0.12**	**0.3**	**0.09**	**0.2**	**0.11**	**0.02**
Apr 08	**7.6 ± 1.3**	**12.1 ± 0.8**	**12.1 ± 1.0**	**12.2 ± 1.8**	**9.4 ± 1.2**	**6.9 ± 0.6**	**8.0 ± 0.8**	**7.5 ± 0.9**	**0.8 ± 0.5**
May 08	**8.6 ± 1.8**	**19 ± 2**	**8.6 ± 0.7**	**9.1± 0.7**	**7.9 ± 1.9**	**8.7 ± 1.7**	**9.1 ± 1.8**	**7.8 ± 1.6**	**0.9 ± 0.7**
Jun08	**8.8 ± 1.5**	**17.6 ± 1.7**	**19 ± 2**	**14 ± 4**	**9 ± 2**	**9.4 ± 1.2**	**8 ± 2**	**7.0 ± 1.4**	**1.2 ± 0.6**
Oct 08	**9.0 ± 0.8**	**14 ± 2**	**11.5 ± 0.8**	**11.3 ± 1.5**	**9.4 ± 1.3**	**7.7 ± 1.0**	**7.6 ± 0.9**	**7.7 ± 0.8**	**0.3 ± 0.3**
Mean 2	**8.6**	**13.8**	**10.8**	**9.9**	**9.1**	**7.5**	**7.9**	**7.5**	**0.6**
StDev 2	**0.6**	**0.6**	**0.4**	**0.6**	**0.7**	**0.4**	**0.5**	**0.5**	**0.2**
Var 2	**0.3**	**0.4**	**0.2**	**0.35**	**0.55**	**0.2**	**0.3**	**0.3**	**0.05**
Nov 08	**6.6 ± 1.8**	No Measure	**13.1 ± 1.1**	No Measure	No Measure	**6.3 ± 0.8**	No Measure	No Measure	**0.4 ± 0.2**
Dec 08	**4.5 ± 0.3**	**7.0 ± 0.6**	**8.9 ± 1.2**	**10 ± 2**	**6.4 ± 1.1**	**5.4 ± 0.6**	**6.2 ± 1.1**	**4.6 ± 1.0**	**0.6 ± 0.3**
Mean 3	**4.6**	**7**	**11.2**	**10**	**6.4**	**5.7**	**6.2**	**4.6**	**0.45**
StDev 3	**0.3**	**0.6**	**0.8**	**2**	**1.1**	**0.5**	**1.1**	**1**	**0.15**
Var 3	**0.08**		**0.65**			**0.25**			**0.03**

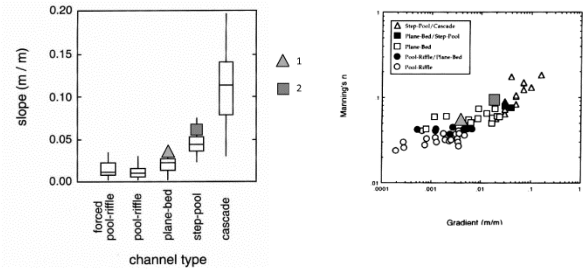

Fig.8 - Classification of the Sicilì Bridge (1) and WWF Oasis reference reaches (2), in relation to: a) longitudinal slope and b) gradient vs. Manning's n.

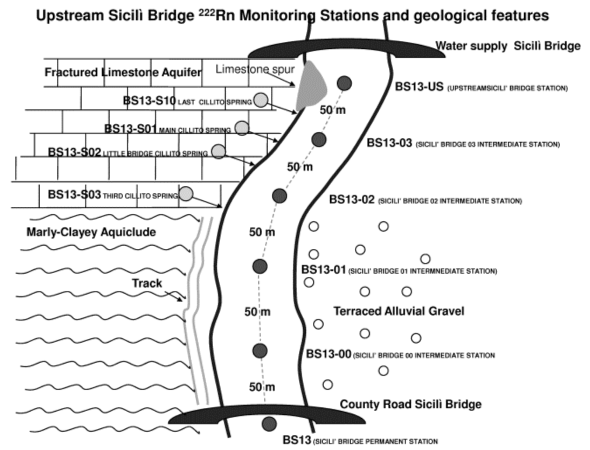

Fig.9 - Radon Monitoring Stations and geological features upstream the Sicilì Bridge.

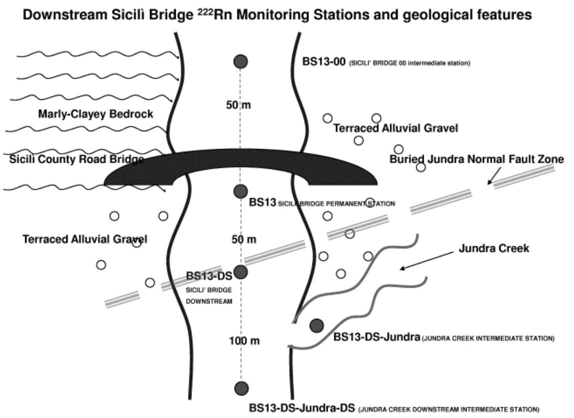

Fig.10 - Radon Monitoring Stations and geological features downstream the Sicilì Bridge.

4.2 River reach scale analysis

The rate of spatial in-stream groundwater influx results differentiated for the two segments of interest, in relation to groundwater hydro-chemical type, discharge magnitude, and hydraulic river constraints, related to hydro-geomorphological typology of stream.

In order to understand this differentiation, due to a different degassing rate in Radon from free surface of streamflow, an analysis at reach level and more detailed scale has been performed along the Sicilì Bridge reference reach and WWF Oasis reference reach. In the following, the results and data discussion for each reach are explained.

Their hydro- geomorphological characteristic, based on standardized geomorphic measurements [88], allow to classify the first reach in the category "plane bed", sensu Montgomery&Buffington, [77], defined as an alluvial channel bed morphology type "C", and the second, in the "step-pool" category with a channel bed morphology type "B".

Figure 8 highlights the relations between the above reaches and their classification, sensu Montgomery&Buffington [77], referring to the main hydraulics parameters (slope/gradient and Manning's n).

4.2.1 Sicilì Bridge reference reach

This reference reach is located uppermost the Middle-lower Bussento river segment (Fig. 3), identified by the reference main station BS13 (Sicilì Bridge).

The station BS13-US has been chosen as an upstream monitoring station. It is placed upstream the Cillito springs group, emerging along the right bank, from enlarged fractures into Miocene calcarenites, overlaid by the marly-clayey formation regional aquiclude.

Downstream, the first spring outlet of the Cillito group, four monitoring secondary stations (BS13-03, BS13-02, BS13-01, BS1300 - have been established in the river at a relative distance of 50 m, one from the other (Fig. 9).

Downstream the main station BS13, other two monitoring stations have been established: BS13-DS, and BS13-DS-Jundra-DS, this one downstream the superficial inflow from Jundra creek (Fig. 10).

The results of the measurement campaigns are reported in Tab. 6 and the associated data are plotted in Fig. 11.

Here, the data from all the stations established along this reach are summarized in the context of the segment to which they belong, and have been classified according to the seasonal period (recharge, discharge) of the measurement campaign, in order to highlight the time variability of the results, with the respect to the spatial variability of the ones reported in Figg. 6 and 7 at the segment scale.

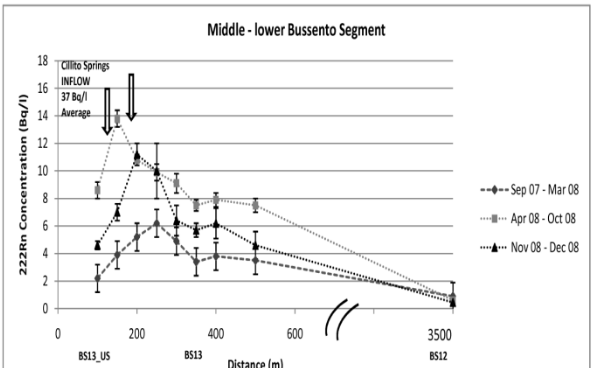

Fig.11- Average Radon activity concentration values measured at the Middle – lower Bussento, divided into three groups according to the different seasonal periods (discharge, recharge).

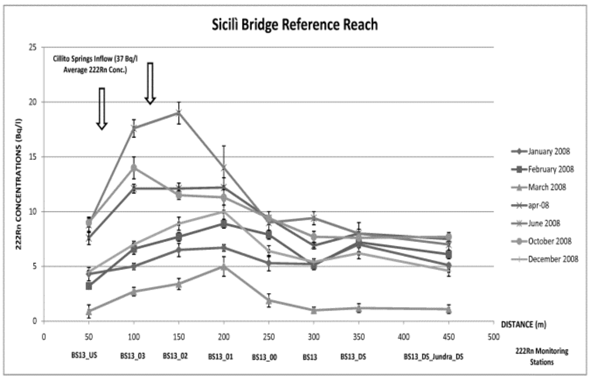

Fig.12- Radon activity concentration values measured (monthly base) at the Sicilì Bridge reference reach.

Tab.7 - Radon degassing coefficient along the Sicilì Bridge reference reach.

Measurement Campaign	Degassing Coefficient α (m^{-1})	R^2 Curve Fitting
January 08	$6.4 \cdot 10^{-4}$	0.961
February 08	$5.1 \cdot 10^{-4}$	0.945
March 08	$4.3 \cdot 10^{-4}$	0.420
April 08	$7.8 \cdot 10^{-4}$	0.968
May 08	$6.4 \cdot 10^{-4}$	0.924
June 08	$7.9 \cdot 10^{-4}$	0.884
October 08	$10.0 \cdot 10^{-4}$	0.990
December 08	$7.7 \cdot 10^{-4}$	0.952

These results show, as expected, that concentration measured at the group of 4 stations from BS13_03 to BS13_00 increases because of the inflow of the lateral springs, whose water is richer in Radon. At the following stations there is a downstream decrease of Radon concentration due to Radon losses to the atmosphere, with the exception of the station BS13_DS, which shows a certain increase of concentration for almost all the measurement campaign.

The plots from Fig. 11 and Fig. 12 also show:

1) Homogeneity in the general trend of the curves: there is, in fact, an increase in Radon activity concentration values starting from the station BS13_03 and then a decrease from the station BS13 which is not influenced by the springs.
2) Seasonality of radon relative concentrations, confirming in general that the measures made during the aquifer recharge period provide values of concentrations that are lower than the ones of the discharge period. There is also an intermediate stripe of values corresponding to the first part of the new recharge period with a decrease in the Radon activity concentration.
3) There is an anomalous increase in Radon concentration, for all the three periods considered,
4) between the stations BS13 and BS13_DS, that is at the moment subject of further investigations in order to determine whether it can be attributed just to statistical fluctuations or not.

An analysis of the Radon diffusion phenomenon from water to atmosphere has been made for the Sicilì segment. We hypothesize that Radon losses due to degassing can be explained by an exponential law, $e^{-\alpha L}$ (2), according to the outcome of the application of the stagnant film model [40, 89], where L is the distance between two stations and α is a decay-like coefficient. So, the station BS13_02, can be considered as the higher point and the station BS12 as the lower one to calculate α for this segment.

The results are reported in Tab. 7 and they show that the estimated value for α is higher in the discharge period (mean value: $8.3 \cdot 10^{-4}$ m^{-1}) than the one for the recharge period (mean value: $5.0 \cdot 10^{-4}$ m^{-1}).

4.2.2 WWF Oasis reference reach

This second case study concerns another reference reach of the Bussento river, located inside a World Wildlife Fund (WWF) oasis (Fig. 13), in which there is a main spring (BS15_S01 – Old Watermill Spring), where an average radon activity concentration of 36.5 Bq/l has been measured.

As in the previous case, a monitoring station (BS15_S01_US – Old Watermill Upstream) has been established above the inflow of the water coming from the spring, which, through a little cascade, falls into the river. Below the cascade and down the course of the river other 4 monitoring stations have been established. This part of the river is characterized by high turbulence, according to the step and pool stream typology, which surely can affects the Radon losses, increasing its degassing to the atmosphere. The results of the measurement campaigns, reported in Tab. 4, are plotted in Fig.14. It can be inferred a great increase in the Radon activity concentration in correspondence of the stations below the spring inflow, and then a quick decrease.

Also for the WWF Oasis reach, a preliminary modeling has been made for the Radon degassing from water: in this case, because of the high turbulence of the river, we have a very sudden and sharp decrease of the Radon activity concentration values as shown in Fig.14. The highest point in the plot (corresponding to the monitoring station BS15_S01_01 below the inflow from the main spring BS15_S01) and the lowest one (corresponding to the last station BS15_S01_DS) have been considered, obtaining that the best curve fitting the plot is a power-law-like $y = K*x^{-\delta}$ (3) with δ as Radon "degassing" coefficient in this case (Fig. 15).

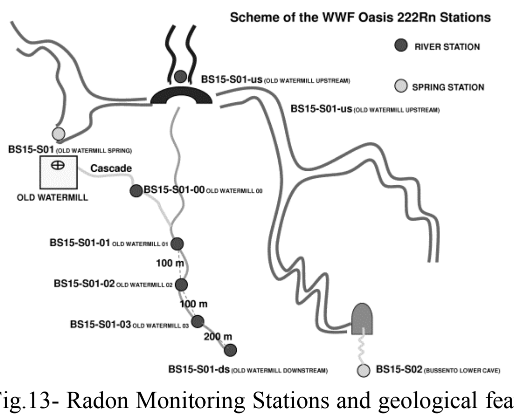

Fig.13- Radon Monitoring Stations and geological features at WWF Oasis reference reach.

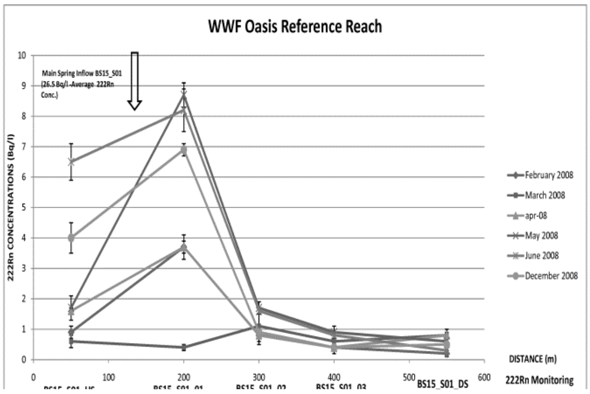

Fig.14 - Radon activity concentration values measured at the WWF Oasis reference reach

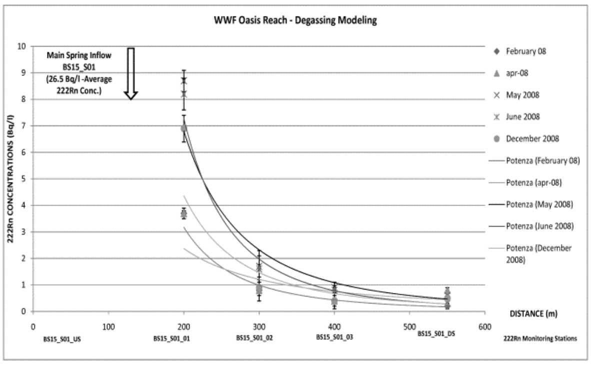

Fig.15 - Radon degassing modeling for the data from the WWF Oasis reference reach

Tab.8 - Radon degassing coefficient along the WWF Oasis reference reach.

Measurement Campaign	Coefficient K [Bq/l*m]	δ	R^2 Curve Fitting
February 08	10^7	2.87	0.979
April 08	$1.6*10^4$	1.66	0.578
May 08	$9*10^6$	2.65	0.938
June 08	$2*10^8$	3.22	0.989
December 08	$7*10^6$	2.69	0.795

4.2.3 Karst spring groundwater analysis

Some karst springs along the Bussento river basin have been, also, monitored. Their importance is due to their content in Radon, which is responsible of the Radon activity concentration increase in the surface water. According to the results in Radon activity concentration, three "families", corresponding to the typologies of karst springs assumed in the conceptual model, have been identified (Tab. 9) :

1) Fracture basal springs (i.e., B13_S01 and BS13_S02), with high values of Radon activity concentration (32.4 Bq/l (mean value) from the first one and 35.8 Bq/l from the second one) and with low standard deviation and variance values;
2) Conduit springs (i.e., BS15_S01) with very variable values (between 17.5 Bq/l (min) and 33.5 Bq/l (max)) and with low standard deviation and variance values;
3) Cave resurgence springs with highly variable values (between 0.5 Bq/l (min) and 6.5 Bq/l (max)).

There is, therefore, a spatial variability in Radon activity concentration, which is shown in figure 16. As for the seasonal variability, the two basal springs of the Cillito group do not show any relevant difference in Radon concentration during the year. At the conduit spring (BS15_S01), more varying values have been obtained: they are a little higher in the recharge period (average value: 26.4 Bq/l) than in the discharge one (mean value: 23 Bq/l). For the resurgence spring some higher values (6.5 Bq/l) have been obtained at the beginning of the discharge period, while in the other months there are data with little variability.

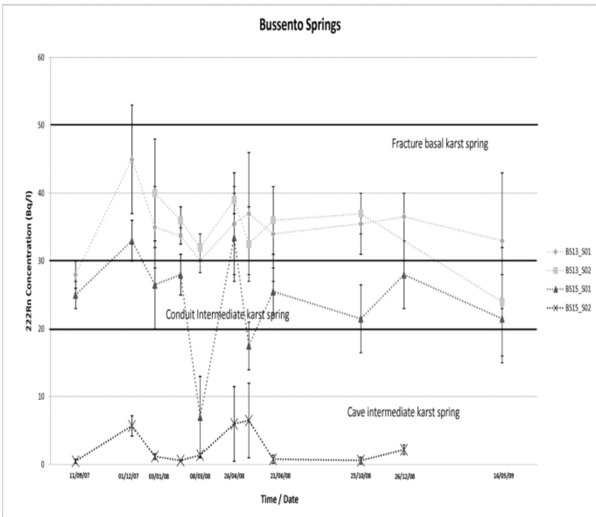

Fig.16 - Seasonal variability of the three "families" of Radon concentration in the Bussento karst springs.

Tab.9 - Data obtained from the measurement at the spring monitoring stations

Spring Station	[^{222}Rn] Min (Bq/l)	[^{222}Rn] Max (Bq/l)	[^{222}Rn] Mean (Bq/l)	DEV ST	VAR
BS13_S01	28	45	32.4	0.8	0.68
BS13_S02	32	40	35.8	1.0	1.05
BS15_S01	17.5	33.5	25.6	1.1	1.20
BS15_S02	0.5	6.5	1.10	0.13	0.017

Tab.10 - Seasonal variability of the three "families" of karst springs according to Radon activity concentration.

STATIONS	BS13_S01 Main Cillito Spring	BS13_S02 Little Bridge Cillito Spring	BS15_S01 Old Watermill Spring	BS15_S02 Bussento Lower Cave
Measurement Campaign	222Rn Concentration (Bq/l)	222Rn Concentration (Bq/l)	222Rn Concentration (Bq/l)	222Rn Concentration (Bq/l)
September 07	28 ± 2	No Measure	25 ± 2	0.5 ± 0.3
December 07	45 ± 8	No Measure	33 ± 3	5.7 ± 1.5
January 08	35 ± 6	40 ± 8	26.5 ± 6.5	1.2 ± 0.4
February 08	33.7 ± 1.2	36 ± 2	28 ± 3	0.6 ± 0.1
March 08	30.1 ± 1.8	32 ± 2	7 ± 6	1.4 ± 0.2
Mean 1	31.9	34.2	26.4	1.1
Dev St 1	0.9	1.4	1.4	0.14
Var 1	0.77	1.93	1.91	0.02
April 08	35.5 ± 7.5	39 ± 2	33.5 ± 6.5	6.0 ± 5.5
May 08	37 ± 9	32.5 ± 5.5	17.5 ± 3.5	6.5 ± 5.5
June 08	34 ± 7	36 ± 5	25.5 ± 3.5	0.8 ± 0.6
October 08	35.5 ± 4.5	37 ± 3	21.5 ± 5.0	0.6 ± 0.5
Mean 2	35	37.7	23	0.7
Dev St 2	3	1.5	2	0.4
Var 2	10	2.3	4.4	0.15
November 08	No Measure	No Measure	No Measure	No Measure
December 08	36.5 ± 3.5	No Measure	28 ± 5	2.2 ± 0.7
Mean 3	36.5		28	2.2
Dev St 3	3.5		5	0.7
Var 3				

5 Conclusions

The implementation of the Radon measurement techniques, along the surface and groundwater bodies in the Bussento river basin, has confirmed the prospective of using these methodologies in a karst Mediterranean environment to investigate the complex interactions and exchanges between streamflow and groundwater.

Experimental data about Radon concentrations, in addition to physical-chemical data and streamflow rate, have been acquired during monthly measurement campaigns. From the subsequent analysis, it has been established the possibility of localizing groundwater influx in riverbed. The data have also enabled to individuate a spatial and temporal variability of the Radon activity concentration along the river, and to identify three typologies of karst springs assumed in the conceptual model. Moreover, a preliminary investigation and modeling of Radon diffusion from water have been made along two selected segments of the river.

The future aim of this research program is to continue and improve these studies using Radon as a naturally occurring tracer in the Bussento river basin, and to extend this investigation to other karst Mediterranean environments in the Campania Region and in the whole Southern Italy.

References:

[1] FAO, Strategies, approaches and systems in integrated watershed management, *Conservation Guide*, 14, Rome, 1986.

[2] FAO, Developing participatory and integrated watershed management, *Community Forestry Case Study Series*, 13, Rome, 1998.

[3] Karanth K., *Groundwater assessment. Development and management*, Tata McGraw-Hill, 1987.

[4] Winter T., Management of groundwater and surface water, *Review of Geophysics*, Supplement 33, 1995.

[5] Marine I. W., The use of naturally occurring helium to estimate groundwater velocities for studies of geologic storage of radioactive waste, *Water Resources and Research*, 15, 1979, 1130-1136.

[6] Tolstikhin I. N. and Kamensky I. L., Determination of groundwater age by the T-3He method, *Geochem. Int.*, 6, 1969, 810-811.

[7] Loucks D. and Gladwell J., *Sustainability criteria for water resource systems*, Cambridge University Press, 1999.

[8] IAEA. Rickwood P., 2002. *IAEA Bulletin*, 44/1/2002, pp. 21-24.

[9] Smith L., Using Radon-222 as a tracer of mixing between surface and ground water in the Santa Fe river sink/rise system. Thesis presented to the graduate school of the University of Florida, 2004.

[10] Dassonville L. and Fé d'Ostiani L., Mediterranean watershed management: overcoming water crisis in the Mediterranean, *Watershed Management: Water Resources for the Future* -Working Paper 9, Chapter 6, Watershed Management & Sustainable Mountain Development Conference Proceedings (Porto Cervo, Sassari, Sardinia, Italy, 22-24 October 2003).

[11] Tulipano L., Fidelibus D., Panagopoulos A., COST Action 621 *Groundwater management of coastal karstic aquifers*, Final report, 2005.

[12] Longobardi A. and Villani P., Baseflow index regionalization analysis in a Mediterranean environment and data scarcity context: role of the catchment permeability index, Journal of Hydrology, 355, 2008, 63-75.

[13] Simonovic S., Water resources engineering and sustainable development, *Proceedings of the XXVI Congress of Hydraulics* (Catania, Italy, 1998).

[14] Shah T., Molden D., Sahthiradelvel, Seckler D., The global situation of groundwater: overview of opportunities and challenges, *International Water Management Institute*, 2001.

[15] EWFD, 2000. Directive 2000/60/EC of the European Parliament and of the Council of 23 October 2000 establishing a framework for Community action in the field of water policy (OJ L 327, 22.12.2000, p. 1). (The EU Water Framework Directive (EWFD) - integrated river basin management for Europe, (http://ec.europa.eu/environment/water/water-framework/index_en.html).

[16] Menéndez M. and Pinero M. J., Common Implementation Strategy for the Water Framework Directive (2000/60/EC) - Guidance Document No 11, Planning Processes Produced by Working Group 2.9 – Planning Processes, Office for Official Publications of the European Communities, Luxembourg: 2003 - ISBN 92-894-5614-0-ISSN 1725-1087.

[17] Grath J., Ward R., Quevauviller P., Common Implementation Strategy for the Water Framework Directive (2000/60/EC), Guidance Document No. 15 – Guidance on Groundwater Monitoring. Publications of the

European Community, Luxembourg ISBN 92-79-04558-X - ISSN 1725-1087.

[18] Ford, D. C. and Williams P. W., *Karst geomorphology and hydrology*, London, Unwin, Hyman, 1989.

[19] Ford, D. C. and Williams, P. W., *Karst Hydrogeology and Geomorphology.* (Reprint with corrections of the 1989 title “Karst geomorphology and hydrology”). J. Wiley and Sons Ltd, Chichester, 2007.

[20] Margat J. and Vallée D., Water Resources and Uses in the Mediterranean Countries. Figures and Facts. *The Mediterranean in Figures. Blue Plan for the Mediterranean.* Regional Activity Centre, Sophia-Antipolis, France, 224 pp., 2000.

[21] Vogel R. M. and Kroll C.N., Regional geohydrologic-geomorphic relationships for the estimation of low-flow statistics, *Water Resources and Research*, 28 (9), 1992, 2451-2458.

[22] Quevauviller PH., 2005. Groundwater monitoring in the context of EU legislation: reality and integration needs, *The Royal Society of Chemistry, J. Environ. Monit.*, 7, 2005, 89–102.

[23] Barbieri, M., Boschetti, T., Petitta, M., Tallini M., Stable isotopes (2H, 18O and 87Sr/86Sr) hydrochemistry monitoring for groundwater hydrodynamics analysis in a karst aquifer (Gran Sasso, Central Italy), *Applied Geochemistry*, 20(11), 2005, 2063-2081.

[24] Brahana J.V., and Hollyday E.F., Dry stream reaches in carbonate terranes – Surface indicators of ground-water reservoirs, *American Water Resources Association*, 24(3), 1988, 577-580.

[25] Vervier P. and Gibert J., Dynamics of surface water/groundwater ecotones in a karstic aquifer, *Freshwater Biol.*, 26(2), 1991, 241-250.

[26] Quartieri J., Troisi A., Guarnaccia C., Lenza T.L.L., D’Agostino P., D’Ambrosio S., Iannone G., An Acoustical Study of High Speed Train Transits, *WSEAS Transactions on Systems*, Issue 4, Volume 8, (2009), pp. 481-490, ISSN: 1109-2777.

[27] Quartieri J., Troisi A., Guarnaccia C., Lenza T.L.L., D’Agostino P., D’Ambrosio S., Iannone G., Application of a Predictive Acoustical Software for Modelling Low Speed Train Noise in an Urban Environment, *WSEAS Transactions on Systems*, Issue 6, Volume 8, (2009), pp.673-682, ISSN: 1109-2777.

[28] Guarnaccia C., Analysis of Traffic Noise in a Road Intersection Configuration, *WSEAS Transactions on Systems*, Issue 8, Volume 9, (2010), pp.865-874, ISSN: 1109-2777.

[29] Levêque P. S., Maurin C., Severac I., Le 222Rn traceur naturel complementaire en hydrologie souterranie, *C. R. Hebd. Seances Acad. Sci.,* 272, 18, 1971, 2290.

[30] McDonnell I. J., Where does water go when it rains? Moving beyond the variable source area concept of rainfall-runoff response, *Hydrological Processes*, 17, 2003, 1869-1875.

[31] Solomon D. K., Schiff S. L., Poreda R. J. and Clarke W. B., A validation of the 3H/3He method for determining groundwater recharge, *Water Resources and Research*, 29, 9, 1993, 2851-2962.

[32] Solomon D. K., Poreda R. J., Cook P. G. and Hunt A., Site characterization using 3H/3He groundwater ages (Cape Cod, MA.), *Ground Water*, 33, 1995, 988-996.

[33] Solomon D. K., Cook P. G., and Sanford W. E.,. Dissolved Gases in Subsurface Hydrology. in: *Isotope Tracers in Catchment Hydrology* (Kendall C. and McDonnell J.J. (Eds.)). Elsevier, 1997, pp. 291-318.

[34] Goldscheider N. and Drew D., *Methods in Karst Hydrogeology.* Taylor & Francis Group, London, 2007, UK.

[35] Emblanch C., Zuppi G.M., Mudry J., Blavoux B., Batiot C., Carbon-13 of TDIC to quantify the role of the unsaturated zone: the example of the Vaucluse karst systems Southeastern France, *Journal of Hydrology*, 279, 2003, 262-274.

[36] Andrews, J. N. and D. F. Woods, Mechanism of radon release in rock matrices and into groundwaters, *Trans. Inst. Min. Metall. Sec.*, B81, 1972, 198-209.

[37] Shapiro M.H., Rice A., Mendenhall M.H., Melvin D. and Tombrello T.A., Recognition of environmentally caused variations in radon time series, *Pure and Appl. Geophys.*, 122, 1984, 309-326.

[38] Rogers A., Physical behaviour and geologic control of radon in mountain streams, *U.S. Geological Survey Bulletin*, 1052 – E, 1958.

[39] Rama and Moore, W. S., Mechanism of transport of U–Th series radioisotopes from solids into ground water, *Geochim. Cosmochim. Acta*, 48, 1984, 395–399.

[40] Ellins, K. K., Roman-Mas A., Lee R., Using 222Rn to examine Groundwater/surface discharge interaction in the Rio Grande de

Manati, Puerto Rico, *Journal of Hydrology*, 115, 1990, 319-341.

[41] Lee R. and Hollyday E. F., Radon measurement in streams to determine location and magnitude of ground-water seepage. in: *Radon, radium, and other radioactivity in groundwater.* (Graves B. (Ed.)), 1987, 241-249. Lewis Publishers, Inc. (Chelsea, Mich.).

[42] Lee R. and Hollyday E. F., Use of radon measurements in Carters Creek, Maury County, Tennessee, to determine location and magnitude of groundwater seepage. in: *Field studies of radon in rocks, soils and water.* (Gundersen, L.C. and Wanty, R.B. (Eds.)), 1991, 237-242. U. S. Geological Survey Bulletin.

[43] Genereaux, D. P., and Hemond, H. F., Naturally occurring radon-222 as a tracer for streamflow generation: steady state methodology and field example, *Water Resources and Resources*, 26 (12), 1990, 3065 - 3075.

[44] Genereaux, D. P., Hemond, H. F., and Mulholland, P. J., Use of radon-222 and calcium as tracers in a three-end-member mixing model for streamflow generation on the wet fork of Walker Branch watershed, *J. Hydrol.*, 142, 1993, 167- 211.

[45] Gudzenko V., Radon in subsurface water studies. In: *Isotopes of Noble Gases as Tracers in Environmental Studies*. Proceedings of a Consultants Meeting, International Atomic Energy Agency, Vienna, 1992, 249-261.

[46] Kraemer T.F. and Genereaux D.P., Applications of Uranium- and Thorium-Series Radionuclides in Catchment Hydrology Studies. in: *Isotope Tracers in Catchment Hydrology* (Kendall C. and McDonnell J.J. (Eds.)). Elsevier, Amsterdam, 1998, 679-722.

[47] Hooper, R.P. and C.A. Shoemaker A comparison of chemical and isotopic streamflow separation, *Water Resour. Res.*, 22 (10), 1986, 1444-1454.

[48] Sultankhodzhaev A. N., Spiridonov A. I., Tyminsij V. G. , Underground water's radiogenic and radioactive gas ratios (He/Rn and Xe/Rn) in groundwaters and their utilization for groundwater age estimation, *Uzbek Geol. J.* 5, 1971,p. 41.

[49] Hoehn E. and von Gunten H. R., Radon in Groundwater: a tool to assess infiltration from surface waters to aquifers, *Water Resources and Research*, 25, 1989, 1795 - 1803.

[50] Hamada H., Estimation of groundwater flow rate using the decay of 222Rn in a well, *Journal of Environmental Radioactivity*, 47, 2000, 1-13.

[51] Hakl J., Hunyadi I., Csige I., Geczy G., Lenart L., Varhegyi A., Radon transport phenomena studied in karst caves: International experiences on radon levels and exposures. *International Conference on Nuclear Tracks in Solids* No. 18, (Cairo , Egypte, 01/09/1996) vol. 28, no. 1-6, 1997, 675 - 684.

[52] Semprini L., Radon-222 concentration in groundwater from a test zone of a shallow alluvial aquifer in the Santa Clara Valley, California. in: *Radon in Groundwater*, (Graves B., (Ed.)). Lewis Publishers, Clelsea, MI, 1987, 205-218.

[53] Gainon F., Goldscheider N., Surbeck H., Conceptual model for the origin of high radon levels in spring waters –the example of the St. Placidus spring, Grisons, Swiss AlpsSwiss, *J. Geosci.*, 100, 2007, 251–262.

[54] KafriU., Radon in Groundwater as a tracer to assess flow velocities: two test cases from Israel, *Environmental Geology*, vol. 40, Issue 3, 2001, 392-398.

[55] Yoneda, M., Inoue, Y., and Takine, N., Location of groundwater seepage points into a river by measurement of 222Rn concentration in water using activated charcoal passive collectors, *Journal of Hydrology*, 124, 1991, 307–316.

[56] Hoehener P., Surbeck H., 222Rn as a tracer for nonaqueous phase liquid in the vadose zone: experiments and analytical method, *Vadose Zone Journal*, 3, 2004, 1276-1285.

[57] Schubert M., Personal Communication, 2008.

[58] Eisenlohr L. and Surbeck H. , Radon as a natural tracer to study transport processes in a karst system. An example in the Swiss Jura, *C.R. Acad. Sci.,* Paris, 321, série IIa, 1995, 761-767.

[59] Surbeck H., Dissolved gases as natural tracers in karst hydrology; radon and beyond. UNESCO Chair “ErdélyiMihály” School of Advanced Hydrogeology, Budapest, Hungary, 22-27 August 2005.

[60] D’Elia, G., Guida M. and Terranova, C., Osservazioni sui fenomeni di deformazione gravitativa profonda nel bacino del fiume Bussento. Campania, *Bollettino Società Geologica Italiana,* 106, 1987, (in Italian).

[61] Iaccarino G., Analisi idrogeologica del base flow annuo del medio Bussento. Motivazioni idrogeologiche, *Boll. Museo Storia Naturale Lunigiana*, 6-7 Aulla, 1987. (in Italian).

[62] Iaccarino G., Guida D., Basso C., Caratteristiche idrogeologiche della struttura carbonatica di Morigerati (Cilento Meridionale), *Memorie Società Geologica Italiana*, 41, 1988, 1065-1077, 2ff., 5 tabb, 1 tav. (in Italian).

[63] Guida, D., Longobardi, A., Ragone G., Villani P., Hydrogeological and hydrological modeling for water resources management in karstic landscape at the basin scale. A case study: the Bussento river basin. 3rd EGU General Assembly, Vienna, Austria, 02-07 April 2006.

[64] Todini E., The ARNO rainfall-runoff model, *Journal of Hydrology*, 175, 1996, 339-382.

[65] Franchini M., Wendling, J. and Obled, C. et al., Physical interpretation and sensitivity analysis of the TOPMODEL, *Journal of Hydrology*, 175, 1996, 293-338.

[66] Burnett W.C., Dulaiova H., Estimating the dynamics of groundwater input into the coastal zone via continuous radon-222 measurement, *Journal of Environmental Radioactivity*, 69, 2003, 21-35.

[67] Burnett W.C., Dulaiova H., Radon as a tracer of submarine groundwater discharge into a boat basin in Donnalucata, Sicily, *Continental Shelf Research*, 26, 2006, 862-873.

[68] Burnett W.C. et al., Quantifying submarine groundwater discharge in the coastal zone via multiple methods, *Science of the Total Environment*, 367, 2006, 498-543.

[69] Schubert M., Schmidt A., Paschke A., Lopez A., Balcazar M., In situ determination of radon in surface water bodies by means of hydrophobic membrane tubing, *Radiation Measurements*, 43, 2008, 111 – 120.

[70] Bisci, C., et al., in: *Landslide Recognition*, 1996, pp. 150-160.

[71] D'Argenio B., Pescatore T. & Scandone P., Schema geologico dell'Appennino meridionale (Campania-Lucania). Atti del Convegno: *Moderne vedute sulla geologia dell'Appennino*. Ac. Naz. Lincei, Quad., 1973, 183.

[72] BonardiG., La Carta Geologica dell'Appennino Meridionale, *Mem. Soc. Geol. It.*, 41. Presented at the Congress of Italian Geological Society, Sorrento, Italy, 1988.

[73] Cammarosano A. et al., Il substrato del Gruppo del Cilento tra il M. Vesalo e il M. Sacro (Cilento, Appennino Meridionale), *Bollettino della Società geologica italiana*, 119 (2), 2000, 395 - 405. (in Italian)

[74] Cammarosano A. et al., Nuovi dati sui flysch del Cilento (Appennino meridionale, Italia). New data on the flysch of the Cilento (Southern Apennines, Italy), *Bollettino della Società geologica italiana*, 123 (2), 2004, 253-273. (in Italian)

[75] Guida, D., Iaccarino G. & Perrone V., Nuovi dati sulla successione del Flysch del Cilento nell'area di M.teCentaurino: relazioni fra Unità Litostratigrafiche, Unità Litotecniche e principali Sistemi Franosi, *Memorie Società Geologica Italiana*, 1988, 41 (in italian).

[76] Lambiase S., Ruggiero A., La forra del Torano (Matese Centrale): un caso di convergenza fra morfogenesi carsica e fluviale. *Atti della Società Toscana di Scienze Naturali – Memorie*, Serie A, Vol. LXXXVII, 1980, 171-192. (in Italian).

[77] Montgomery D. R. and Buffington J. M., Channel processes, classification, and response. In: *River Ecology and Management* (Naiman R.J. and Bilby R.E., Eds.), 1998, Springer Verlag.

[78] Burbank, D. W. and Anderson, R. S., *Tectonic Geomorphology*, Malden, MA. Blackwell Publishing, 2001.

[79] White W. B., Conceptual models for limestone acquifers, *Groundwater*, 7 (3), 1969, 15-21.

[80] White W. B., . Conceptual models for carbonate acquifers: revised. In: *Hydrologic Problems in Karst Terrain* (Dilamarter, R. R. and Casallany, S. C. (Eds)). WesternKentuckyUniversity, Bowling Green, KY, 1977, 176-187.

[81] White, W. B., *Geomorphology and hydrology of karst terrains*, OxfordUniversity Press, 1988, Oxford.

[82] White W. B., Conceptual models for karstic aquifers. re-published from: *Karst Modeling: Special Publication* 5 (Palmer A.N., Palmer M.V., and Sasowsky I.D. (Eds.)). The Karst Waters Institute, Charles Town, West Virginia (USA), 2003, 11-16.

[83] Bakalowicz M., The infiltration zone of karst aquifers, *Hydrogeologie*, 4, 1995, 3-21.

[84] Guida M. and Guida D., SGDCILERAD. "Submarine Groundwater Discharge assessment on the interregional coastal areas of Cilento, southern Italy, with measurements of natural isotopic tracers like Radon-222.". Programme "PEOPLE" - Call FP7-PEOPLE-2007-4-2-IIF –Proposal N° 221278, 2007.

[85] Guida, D., Guida, M., Luise, D., Salzano, G., Vallario, A., Idrogeologia del Cilento (Campania), *Geologica Romana* – Vol. XIX, 1980, 349-369.

[86] DURRIDGE, RAD7 RADON DETECTOR. Owner's Manual (Bedford, MA.), 2012, USA.

[87] DURRIDGE, RAD7 RADH20 Radon in Water Accessory. Owner's Manual (Bedford, MA.), 2012, USA.

[88] Nickolotsky A., and Pavlowsky R., Morphology of step-pools in a wilderness headwater stream: The importance of standardizing geomorphic measurements, *Geomorphology,* 83, 2007, 294–306.

[89] Wu Y., Wen X. and Zhang Y., Analysis of the exchange of groundwater and river water by using Radon-222 in the middle HeiheBasin of northwesternChina, *Environmental Geology*, 45(5), 2004, 647–653.